

Correlated Surface Roughening During Photoresist Development

Chris A. Mack
Lithoguru.com, 1605 Watchhill Rd, Austin, TX 78703

Abstract

BACKGROUND: Previous simulation work has shown that uncorrelated Gaussian randomness in the development rate produces surface roughness in a resist that obeys Family-Viscek scaling in the KPZ universality class. However, more rigorous mesoscale simulations produce anomalous scaling.

METHODS: Using a stochastic resist simulator, the dynamical roughness behavior of resist development in 2D is studied with various amounts of correlation in the underlying development rate randomness.

RESULTS: For length scales greater than about 5ξ (the correlation length of the underlying randomness), the dynamical roughness behavior obeys standard Family-Viscek scaling within the KPZ universality class. For length scales on the order of a few ξ or less, the mixed correlations of both ξ and ξ_{\parallel} make the results anomalous.

CONCLUSIONS: It appears that correlations can explain at least some of the anomalous scaling behavior observed previously through the use of mesoscale simulations. Simple scaling relationship can still apply, however, over appropriate length scales.

Keywords: stochastic simulation, resist development, dynamical scaling, line-edge roughness, LER, LWR

1. Introduction

Stochastic models of lithography consider fundamental events such as the absorption of a photon or the chemical reaction of a molecule as stochastic events. As such, these events are described probabilistically, with the mean-field “rate” equation describing the probability that the event occurs. Of course, such a probabilistic description will not make deterministic predictions – instead, quantities of interest will be described by their probability distributions, which in turn are characterized by their moments, such as the mean and variance. While stochastic modeling has been successfully applied to photoresist exposure and post-exposure bake (PEB) processes in recent years^{1,2,3,4,5} the stochastic behavior of resist dissolution is much less understood. Ultimately, the final result will be a roughness of the resist feature sidewalls that leads to line-edge roughness (LER) and line-width roughness (LWR) of the resist feature.

Since the final LER of a high-resolution lithographic feature will include all resist and aerial image contributions, studying LER to extract the contribution of just resist development can be difficult. A simpler approach is to remove the aerial image from the experiment and study the resist surface roughness after a uniform open-frame exposure and development. The use of surface roughness after open-frame exposure and development as a probe for understanding the stochastic nature of resist development will be examined in detail in this paper.

In previous work,^{6,7,8} the concepts of dynamical scaling in the study of kinetic roughness were applied to the problem of photoresist development. Uniform, open-frame exposure and development of photoresist corresponds to the problem of quenched noise and the etching of random disordered media. Using simulations of photoresist development in 1+1 and 2+1 dimensions, the resulting kinetic roughness was shown to fall in the Kadar-Parisi-Zhang (KPZ) universality class for the case of fast development. This paper will extend this previous work in several new ways.

First, simulations using correlated development rate noise (rather than the uncorrelated noise of previous work) will show whether kinetic roughness during development dominates the final lithographic roughness or whether the underlying development rate noise, coming from earlier stochastic processes such as exposure and reaction-diffusion, controls the final surface characteristics. Second, by slowing down the mean development rate while keeping the noise term high, simulations will indicate whether the KPZ class holds in this regime or a different universality class is needed (if one even exists).

2. Correlations in the Development Rate

Dissolution rate uncertainty will inevitably result from uncertainty in the underlying inhibitor concentration (for example, the concentration of protecting groups in a chemically amplified resist). Consider a simple development rate function⁹

$$r(m) = r_{max} \frac{(a+1)(1-m)^n}{a+(1-m)^n} + r_{min}, \quad a = \frac{(n+1)}{(n-1)} (1-m_{th})^n \quad (1)$$

where r is the development rate, m is the relative protecting group concentration, and r_{max} , r_{min} , n , and m_{th} are model parameters. Here, we will neglect r_{min} as small compared to the development rate in the region of interest. The edge of a photoresist feature will necessarily have a protection level near the knee of the development rate curve, so that $m > m_{th}$. Thus, if $n \gg 1$, the development rate in this region will be well approximated by

$$r(m) \approx r'_{max} (1-m)^n, \quad r'_{max} = r_{max} \frac{a+1}{a} \quad (2)$$

This development rate expression will be used throughout this paper. While simple, it accurately reflects the non-linear development rate response for exposure and deprotection levels expected near a photoresist edge.

Suppose that m is a random variable with a normal distribution, so that $m \sim N(\mu, \sigma_m)$. Further suppose that nearby grid points in a simulation volume are correlated. In order to simulate the impact of dissolution one must first define this correlation, using either an autocovariance function for $m(x,y,z)$, or, equivalently, its power spectral density (PSD). The two functions are related by a Fourier Transform. In a previous study,¹⁰ the autocorrelation function of the effective acid concentration during PEB for a chemically amplified resist ($\tilde{R}_{H_{eff}}$) was described.

$$\tilde{R}_{H_{eff}}(\tau) = \frac{\int_{-\infty}^{\infty} R_{PSF}(r) R_{PSF}(r+\tau) dr}{\int_{-\infty}^{\infty} [R_{PSF}(r)]^2 dr} \quad (3)$$

where the reaction-diffusion point spread function (R_{PSF}) has analytical forms in one, two and three dimensions.

While the integrals in equation (3) cannot be carried out analytically in any dimension, the Fourier Transform of equation (3) can, yielding the PSD. Interestingly, performing the calculations produces the same PSD, to within a scale factor, for one, two and three dimensions.

$$PSD(f) = PSD(0) \left(\frac{1 - e^{-(\pi \xi f)^2}}{(\pi \xi f)^2} \right)^2 \quad (4)$$

where the correlation length-like parameter ξ is related to the acid diffusion length σ_D by $\xi = \sqrt{2}\sigma_D$. The zero frequency PSD is calculated from Parseval's theorem.

$$\begin{aligned} \text{1D: } PSD(0) &= \frac{3\sqrt{\pi} \xi \sigma_{H,eff}^2}{8(\sqrt{2}-1)} \approx 1.60466 \xi \sigma_{H,eff}^2 \\ \text{2D: } PSD(0) &= \frac{\pi \xi^2 \sigma_{H,eff}^2}{2 \ln 2} \approx 2.26618 \xi^2 \sigma_{H,eff}^2 \\ \text{3D: } PSD(0) &= \frac{\pi^{3/2} \xi^3 \sigma_{H,eff}^2}{4(2-\sqrt{2})} \approx 2.37643 \xi^3 \sigma_{H,eff}^2 \end{aligned} \quad (5)$$

There is no universally accepted definition of correlation length (L_{corr}) that can pin down its value except to within a multiplicative factor. One definition, for example, is based on the frequency which reduces the PSD by a factor of 2.

$$PSD\left(f = \frac{1}{2\pi L_{corr}}\right) = \frac{PSD(0)}{2} \quad (6)$$

By this definition, the correlation length of the reaction-diffusion system is related to ξ by $L_{corr} = 0.5819\xi = 0.8229\sigma_D$ (for 1D, 2D, and 3D). Another common definition, proposed by Stratonovich¹¹, is the mean value of the autocorrelation function.

$$L_{corr} \equiv \int_0^\infty \tilde{R} dr = \frac{1}{\sigma^2} \int_0^\infty \mathcal{F}^{-1}\{PSD\} dr \quad (7)$$

where the autocorrelation function is assumed to be an even function of the distance r . The second integral can be simplified by changing the order of integration, giving a result that depends on the dimensionality of the problem.

$$\begin{aligned} \text{1D: } L_{corr} &= \frac{PSD(0)}{2\sigma^2} \\ \text{2D: } L_{corr} &= \frac{1}{\sigma^2} \int_{-\infty}^\infty PSD df \\ \text{3D: } L_{corr} &= \frac{1}{\sigma^2} \int_{-\infty}^\infty f PSD df \end{aligned} \quad (8)$$

Carrying out these calculations for the reaction-diffusion PSD,

$$\begin{aligned}
1D: \quad L_{corr} &= \frac{3\sqrt{\pi}}{16(\sqrt{2}-1)} \xi \approx 0.80233\xi \\
2D: \quad L_{corr} &= \frac{PSD_{2D}(0)}{PSD_{1D}(0)} = \frac{4\sqrt{\pi}(\sqrt{2}-1)}{3\ln 2} \xi \approx 1.41225\xi \\
3D: \quad L_{corr} &= \frac{PSD_{3D}(0)}{PSD_{2D}(0)} = \frac{\sqrt{\pi} \ln 2}{2(2-\sqrt{2})} \xi \approx 1.04865\xi
\end{aligned} \tag{9}$$

Thus, depending on the definition used and the dimensionality of the problem, the correlation length is between 0.58ξ and 1.41ξ . For the remainder of this paper, I will use the term correlation length for the reaction-diffusion system as being synonymous with the parameter ξ .

The relationship between the effective acid concentration (H_{eff}) and the relative concentration of protecting groups in the chemically amplified resist (m) is exponential, making calculation of the PSD for m difficult. To simplify matters here, we will assume that the effective acid concentration near the resist line edge is sufficiently small that a linear approximation to the exponential relationship is reasonable. Thus, the relative protecting group concentration will have a PSD of the same form as equations (4) and (5), where the variance of the effective acid concentration is replaced by the variance of the relative protecting group concentration, σ_m^2 . To use this PSD in development simulations, a method of generating correlated random development rates must be used, as described in the next section.

3. Numerically Generating Random Rough Volumes of Development Rate

Given a normally distributed random variable $m \sim N(\mu, \sigma_m)$ and a desired PSD, how does one generate a random volume of $m(x,y,z)$ on a regular grid? While there are several methods available, I prefer the approach proposed by Thorsos.¹² The goal is to create a grid of random numbers with a Gaussian distribution and with spatial correlations that would produce, on average, a given PSD. Thorsos described the algorithm in one dimension, which will be reproduced briefly here. Given N_x grid points with spacing Δx covering a distance $L_x = N_x \Delta x$, the relative protection concentration at the point $x_n = n \Delta x$ is given by

$$m(x_n) = \mu + \frac{1}{L_x} \sum_{j=-N_x/2}^{N_x/2-1} F(f_j) e^{i2\pi f_j x_n} \tag{10}$$

where this calculation is performed as the Fast Fourier Transform (FFT) of F on a grid of frequencies $f_j = j/L_x$. The function F , in turn, is calculated from the amplitude of the PSD (for $j \geq 0$):

$$F(f_j) = \sqrt{L_x PSD(f_j)} \begin{cases} (\eta_1 + i\eta_2)/\sqrt{2} & , j \neq 0, N_x/2 \\ \eta_1 & , j = 0, N_x/2 \end{cases} \tag{11}$$

where η_1 and η_2 are two independent $N(0,1)$ random numbers. Since $m(x_n)$ must be real, the negative frequencies of F are obtained from a symmetry relationship: $F(f_{-j}) = F^*(f_j)$.

The Thorsos algorithm can easily be extended to two and three dimensions, so long as care is taken to properly produce the boundary conditions (a purely real random number is used at the origin and at the outer edges of the volume) and the symmetry to result in a purely real m . In two dimensions, this requires

$$\begin{aligned}
 \operatorname{Re}\{F(f_x, f_y)\} &= \operatorname{Re}\{F(-f_x, -f_y)\} \\
 \operatorname{Re}\{F(-f_x, f_y)\} &= \operatorname{Re}\{F(f_x, -f_y)\} \\
 \operatorname{Im}\{F(f_x, f_y)\} &= -\operatorname{Im}\{F(-f_x, -f_y)\} \\
 \operatorname{Im}\{F(-f_x, f_y)\} &= -\operatorname{Im}\{F(f_x, -f_y)\}
 \end{aligned} \tag{12}$$

In three dimensions,

$$\begin{aligned}
 \operatorname{Re}\{F(f_x, f_y, f_z)\} &= \operatorname{Re}\{F(-f_x, -f_y, -f_z)\} \\
 \operatorname{Re}\{F(-f_x, f_y, f_z)\} &= \operatorname{Re}\{F(f_x, -f_y, -f_z)\} \\
 \operatorname{Re}\{F(f_x, -f_y, f_z)\} &= \operatorname{Re}\{F(-f_x, f_y, -f_z)\} \\
 \operatorname{Re}\{F(f_x, f_y, -f_z)\} &= \operatorname{Re}\{F(-f_x, -f_y, f_z)\} \\
 \operatorname{Im}\{F(f_x, f_y, f_z)\} &= -\operatorname{Im}\{F(-f_x, -f_y, -f_z)\} \\
 \operatorname{Im}\{F(-f_x, f_y, f_z)\} &= -\operatorname{Im}\{F(f_x, -f_y, -f_z)\} \\
 \operatorname{Im}\{F(f_x, -f_y, f_z)\} &= -\operatorname{Im}\{F(-f_x, f_y, -f_z)\} \\
 \operatorname{Im}\{F(f_x, f_y, -f_z)\} &= -\operatorname{Im}\{F(-f_x, -f_y, f_z)\}
 \end{aligned} \tag{13}$$

The random development rate is produced by putting the random value of m for each grid point into equation (2). As a first step, the resulting volume of random development rates were analyzed by extracting its PSD. Since the result is inherently spherically symmetric (dictated by the symmetry of equation (4)), the PSD as a function of the three spatial frequency dimensions was interpolated onto one radial-direction grid. This provides an added benefit of significant averaging for high spatial frequencies (though none for the lowest frequency). Example development rate PSDs, in two and three dimensions, are shown in Figure 1 ($r_{max} = 200$ nm/s, $m_{th} = 0.5$, and $n = 10$).

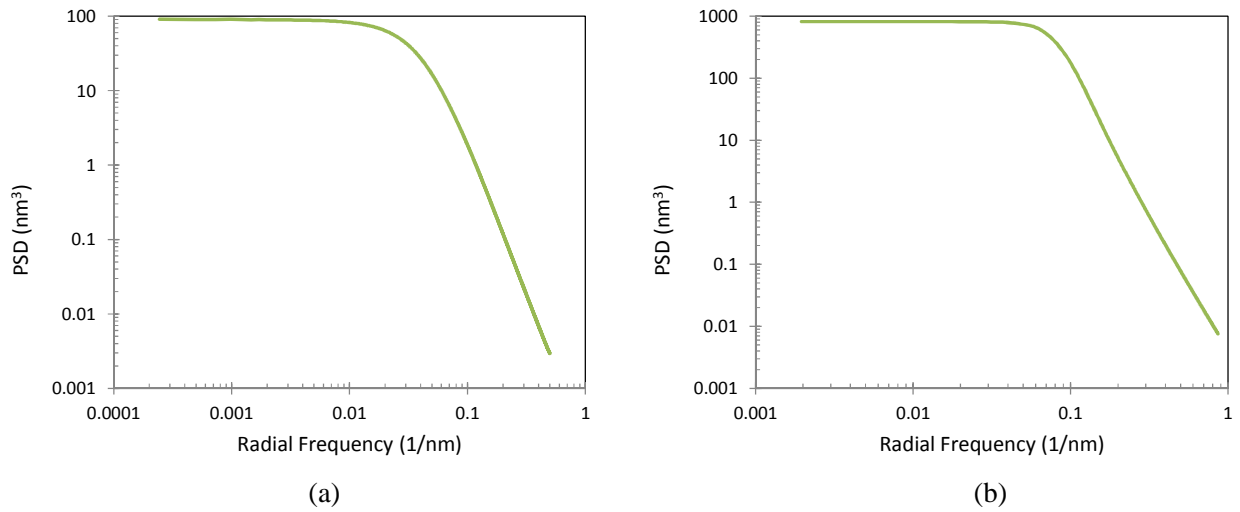


Figure 1. Example power spectral densities of development rates generated by the procedure presented in this paper ($\mu = 0.73$, $\sigma_m = 0.03$, 1000 trials averaged together), for (a) two-dimensions, and (b) three dimensions.

The shapes of the resultant development rate PSDs are similar to, but not exact the same as, the PSD function of equation (4). By fitting this equation to the numerical results, the impact of the highly nonlinear development rate function is seen to be a small decrease in the correlation length as a function of the development nonlinearity, n , multiplied by the relative noise in the protecting group concentration, $\sigma_m/(1-\mu)$. Figure 2 shows these results, along with a quadratic fit to the data.

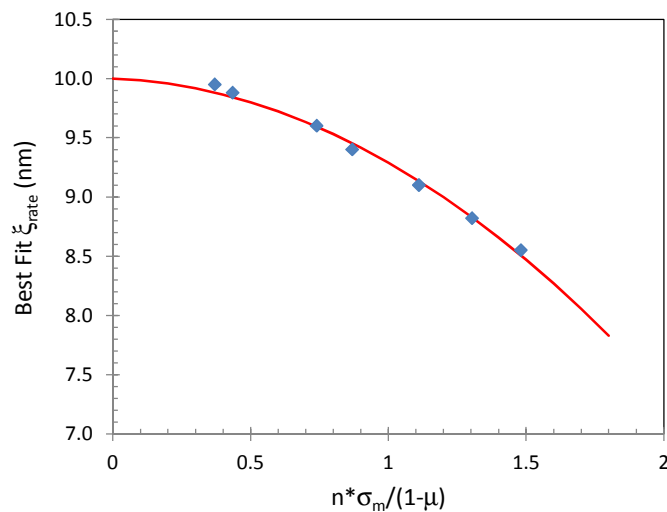


Figure 2. After calculating the development rate PSD in three dimensions (using a correlation length of 10 nm for the protecting group concentration), an estimate of the resulting correlation length was made by fitting to equation (4), shown as the data points. A quadratic fit to the data is also shown.

4. Simulation Results

Using a development volume generated with the proper statistical properties (including the proper correlations), simulations were carried out to predict the resist height as a function of development time for an open-frame exposure/development in the presence of this stochastic dissolution-rate noise. For 3D (2+1) simulations, the grid size was set to 1 nm, simulation widths in x and y were 511 nm, and the resist thickness was 511 nm. The parameters were $r_{max} = 200$ nm/s, $m_{th} = 0.5$, and n was varied between 5 and 15. The development time was adjusted in each case so that approximately 1000 time steps would allow the front to reach the bottom of the resist. For each combination of μ and σ_m evaluated, the development front propagation rate was determined by fitting the average resist surface height versus time with a straight line. An example of 3D simulation results are shown in Fig. 3.

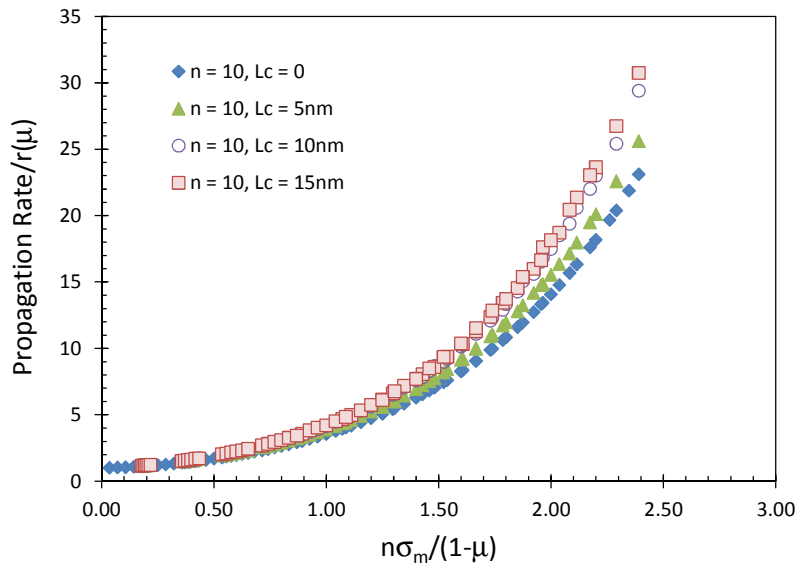


Figure 3. Calculation of the mean propagation rate of the development front in 3D for $n = 10$ and for various correlation lengths (L_c) of m . Each data point is the average of 4 trials.

In addition to investigating mean propagation rates of a development front, the change in surface roughness with development time was investigated using an approach called *dynamical scaling*.^{6,7} The RMS surface height difference, often called the *interface width* or the *surface roughness*, of a statistically self-affine surface scales with the measurement length L as

$$\sigma_w \propto L^\alpha \quad (14)$$

where α is called the *roughness exponent*. Resist surfaces are self-affine only over a region smaller than the correlation length of the roughness. Also, as development proceeds, stochastic effects lead to an increased roughening of the surface. Thus, the statistical properties of the interface are a function of time. Empirically, many problems in etching and deposition show a roughness that, for moderately small times, grows as

$$\sigma_w \propto t^\beta \quad (15)$$

where β is called the *growth exponent*. The growth in roughness as development proceeds does not continue indefinitely. For a given measurement size L , the interface roughness saturates after a long enough time. However, since the roughness varies with L according to equation (14), the point of saturation with development time depends on the size of the measurement region. The overall scaling, called Family-Viscek scaling, can be summarized as¹³

$$\sigma_w \propto L^\alpha f\left(\frac{t}{L^z}\right) \quad (16)$$

where

$$f(u) = \begin{cases} u^\beta & u \ll 1 \\ 1 & u \gg 1 \end{cases}$$

and $z = \alpha/\beta$ is called the *dynamic exponent*. The proper choice of α and β allows dynamic roughness data [$\sigma_w(L,t)$] to collapse to a single universal curve for all L , giving a very sensitive method for determining these exponents.

The dynamic exponent controls the increase in surface roughness correlation (also called the parallel correlation length, ξ_{\parallel}) with development time. If, due to random fluctuations, one point in the resist interface develops down more quickly than the rest, this dimple in the resist surface will begin to spread laterally. Thus, the neighboring points on the interface will have a resist height that is correlated with the original fast-developing point. Initially, this x - y plane correlation length is small, but it grows with time as

$$\xi_{\parallel} \propto t^{1/z} \quad (17)$$

Previous work showed that Family-Viscek scaling accurately described photoresist development when the development rate uncertainty was Gaussian and uncorrelated, with results that fit perfectly into the KPZ universality class.^{6,7} However, Constantoudis *et al.* showed that Family-Viscek scaling did not apply to 2D simulations using a physically-based mesoscale simulator.⁸ Thus, one goal of this work is to explore the cause of the anomalous scaling observed by Constantoudis using a simpler simulation framework.

First, uncorrelated random variation in the protecting level with $m \sim N(\mu, \sigma_m)$ was used to generate random values of dissolution rate at each grid point by insertion into equation (1). Simulation and analysis as described previously was applied to generate dynamic surface roughness data across multiple length scales.^{6,7} Figure 4 shows the resulting surface roughness as a function of development time, and the results of Family-Viscek scaling, for 2D (1+1) simulations (2048 X 2048 grid points). The Family-Viscek scaling works very well to collapse the data using $\alpha = 0.48$ and $\beta = 0.33$, very close to the 2D KPZ values of 1/2 and 1/3, respectively. The data shown is for $n = 5$, but the $n = 10$ results are similar. Note that the first few time steps (corresponding to about 9 seconds and 8 nm of resist removed) do not match the Family-Viscek scaling as well as the rest of the data, giving the small “tails” flaring away from the collapsed curve shown in Fig. 4b.

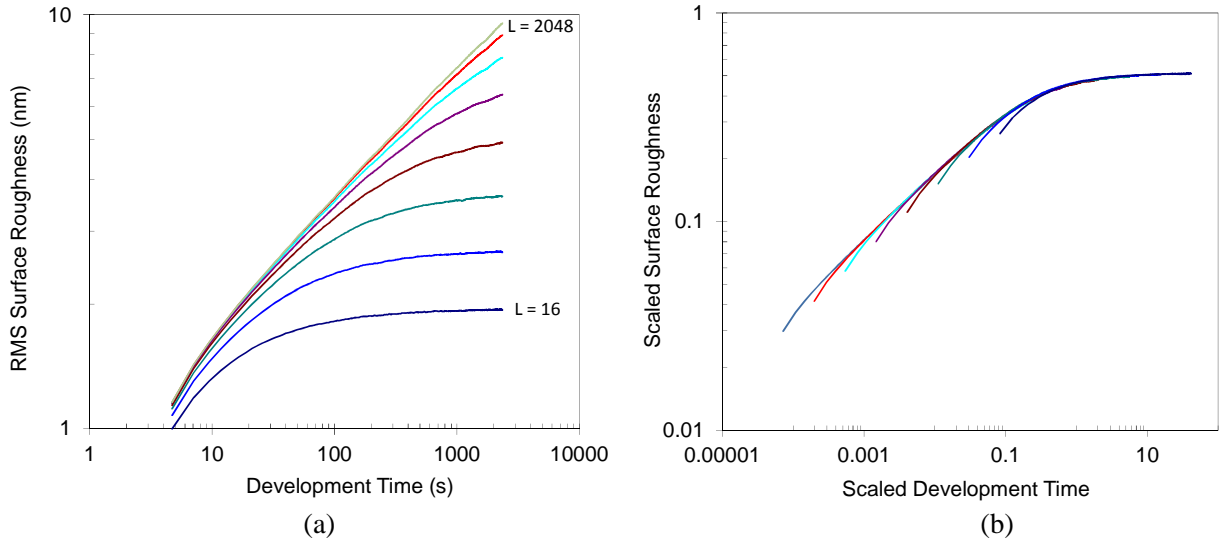


Figure 4. Two-dimensional dynamical simulations of surface roughness with uncorrelated random protecting group concentrations and $n = 10$. a) Raw data, and b) scaled with Family-Viscek using $\alpha = 0.48$, and $\beta = 0.33$. Data shown is the average of 1600 trials.

Examining the power spectral density of the resist surface at different development times also provides insight into the dynamic roughening process. Figure 5a shows the resist surface PSD under the same conditions as Figure 4, for development times starting at 23.6 s in increments of 23.6 s. The parallel correlation length of the resist surface was estimated by fitting each of these curves to a PSD expression inspired by the reaction-diffusion PSD of equation (4), adding an adjustable exponent, s .

$$PSD(f) = PSD(0) \left(\frac{1 - e^{-(\pi \xi_{\parallel} f)^2}}{(\pi \xi_{\parallel} f)^2} \right)^s \quad (18)$$

Each curve was well fit using $s = 0.93$, giving a value for the roughness exponent of $\alpha = 0.43$. An example fit is shown in Figure 5b.

By plotting the resulting correlation length as a function of development time, the scaling exponent z can be obtained from equation (17). The result is shown in Figure 6, producing $z = 1.42$. Using $\alpha = 0.43$, this gives $\beta = 0.30$ (close to the values obtained by finding the best collapse of the scaled roughness data).

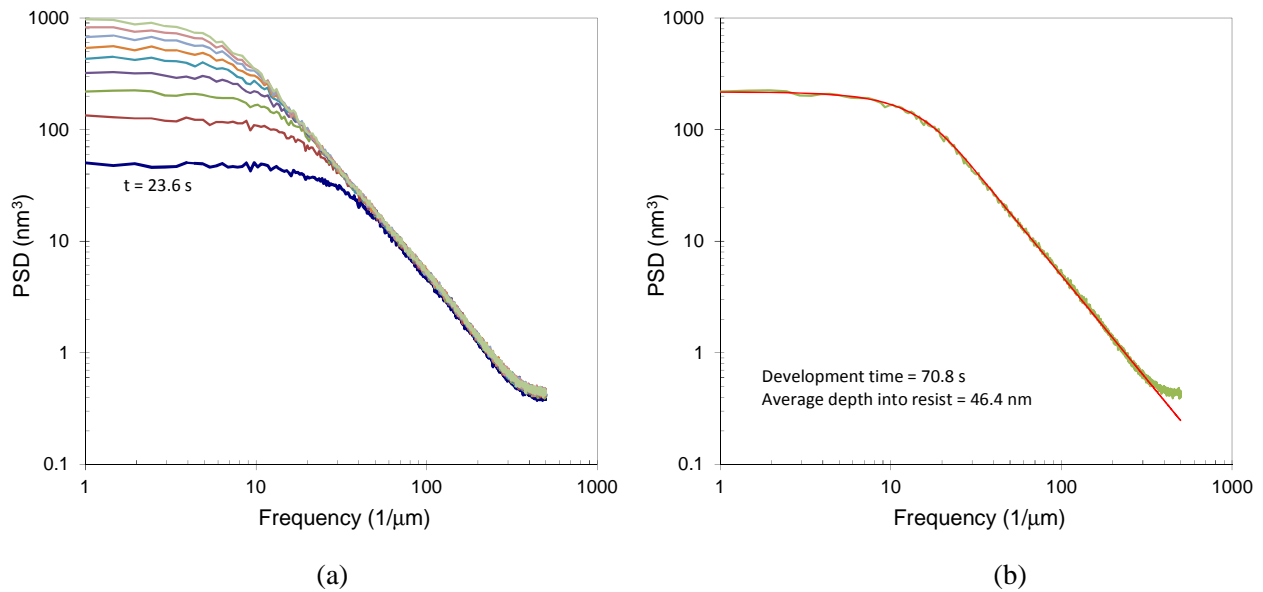


Figure 5. Two-dimensional dynamical simulations of surface roughness with uncorrelated random protecting group concentrations and $n = 10$. a) PSD at development times in increments of 23.6 s, and b) fit of the PSD data for $t = 70.8 \text{ s}$ shown as the thin red line. Data shown is the average of 800 trials.

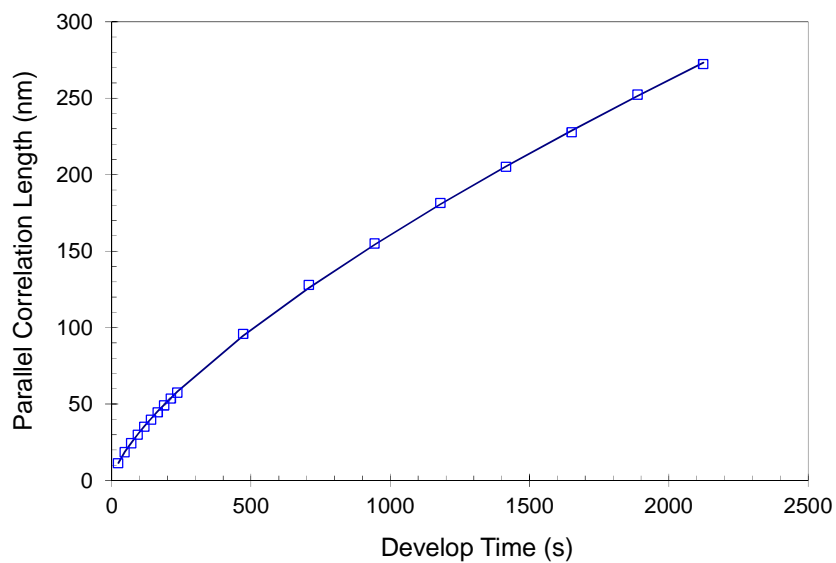


Figure 6. Analysis of the PSDs as shown in Figure 5, as well as those generated for other development times, shows the growth in the parallel correlation length with development time (symbols). A fit to the scaling law is shown as the solid line.

Next, correlation was added to the random protecting group concentrations using the approach discussed above. Correlation lengths between 5 and 30 nm were used with $n = 5$ and 10, and with $\mu = 0.73$

and $\sigma_m = 0.03$. Figure 7 shows the dynamical roughness data (for 1+1 simulations), along with an attempt at Family-Viscek scaling using $\alpha = 0.48$, and $\beta = 0.33$. From the unscaled data for $L = 2048$ in Figure 5a, it is clear that the roughness grows more quickly during the first 20 seconds or so of development, then slows. During this early part of the development, $\beta \approx 0.75$ when $\xi = 5$ nm, $\beta \approx 0.92$ when $\xi = 15$ nm, and $\beta \approx 1.0$ when $\xi = 30$ nm. In the later part of development, β approaches the KPZ value of 0.33. Note that, according to Figure 2, the development rates will have a correlation length that is 90% of the protecting group correlation length when $\mu = 0.73$, $\sigma_m = 0.03$, and $n = 10$.

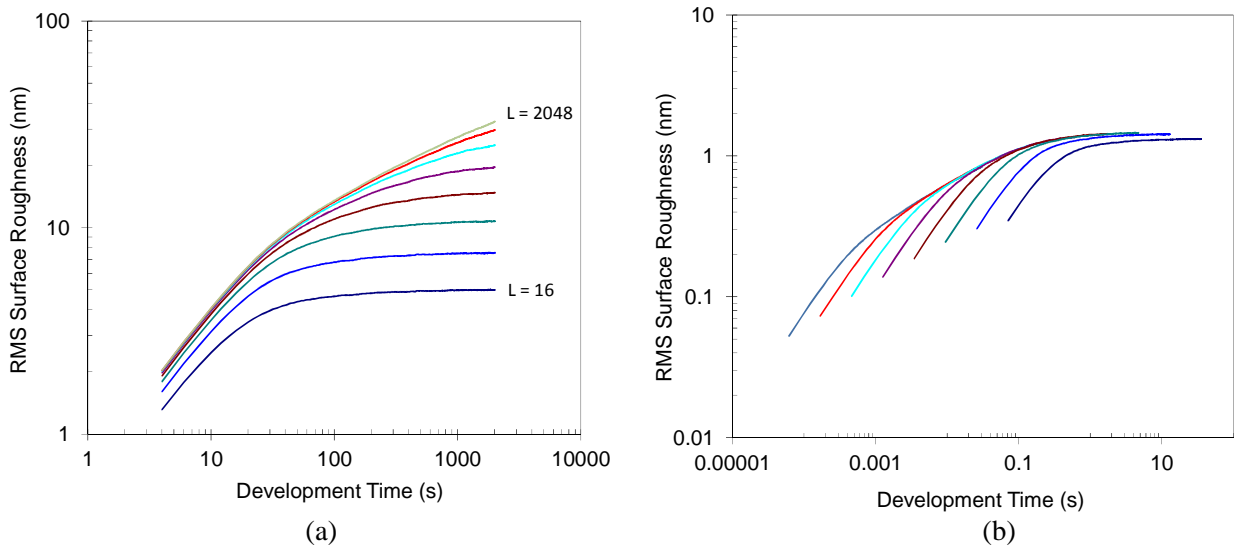


Figure 7. Two-dimensional dynamical simulations of surface roughness with correlated random protecting group concentrations ($\xi = 5$ nm) and $n = 10$. a) Raw data, and b) scaled with Family-Viscek using $\alpha = 0.48$, and $\beta = 0.33$. Data shown is the average of 1000 trials.

Also, this initial development shows a slower progression of the development front from the mean development rate to a “steady state” front propagation rate. Figure 8 shows the front propagation rate (the rate at which the average surface height moves downward) as a function of depth into the resist for different correlation lengths for the protecting group concentration. For all cases, the front propagation rate begins at the mean dissolution rate $\langle r \rangle$ (which was 0.57 nm/s in this case), staying at about this rate until it reaches a depth into the resist equal to about 2/3 of the development rate correlation length. The front propagation rate then grows to a steady-state front propagation rate (0.84 nm/s here), and the transition takes considerably longer as the underlying uncertainty becomes more correlated. Using a $1/e$ criterion, the data from Figure 8 shows that uncorrelated randomness in the development rate requires about 5 nm of depth into the resist to approach the steady state front propagation rate, and the cases of correlated randomness require a depth into the resist equal to about five correlation lengths.

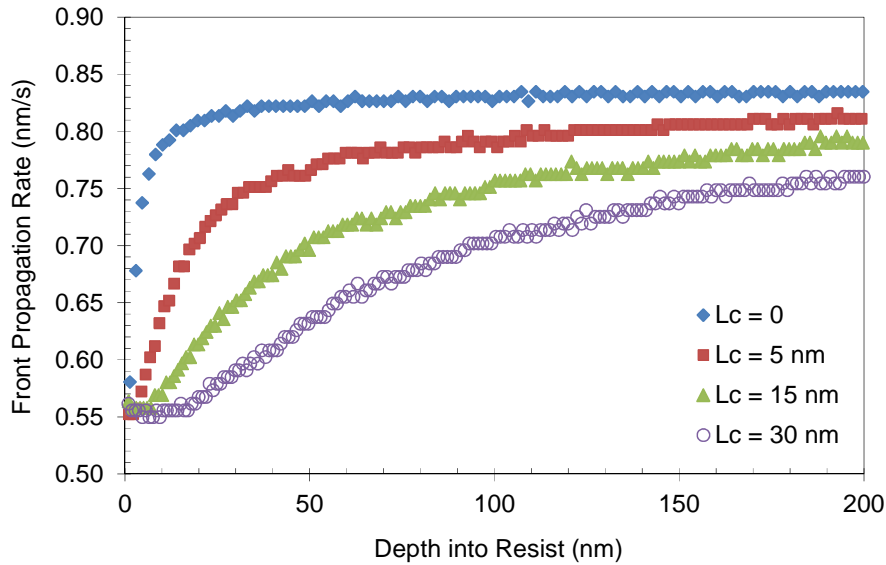


Figure 8. The average front propagation rate increases with depth into the resist (shown here for $\mu = 0.73$, $\sigma_m = 0.03$, and $n = 10$ and for correlation lengths from 0 to 30 nm). Data shown is the average of 1000 trials.

If this initial portion of the simulation is excluded, the remaining dynamic roughening more closely follows Family-Viscek scaling with the KPZ exponents. Figure 9 shows the results when $\mu = 0.73$, $\sigma_m = 0.03$, $n = 10$, and the protecting group correlation length is 15 nm. The first 80 nm (out of a resist thickness of 2047 nm) of data were removed. All but the $L = 16, 32,$ and 64 nm length scales collapse (approximately) onto one curve. Thus, at all length scales greater than about five development rate correlation lengths, the dynamic roughening obeys Family-Viscek scaling in the KPZ universality class. For length scales less than this (both parallel to and perpendicular to the moving resist surface), the scaling remains anomalous. Similar results were obtained with an underlying correlation length of 5 nm, showing KPZ scaling at length scales above about 25 nm.

The reason for the anomalous scaling is the mixture of two sources of correlation along the resist surface. At first, the roughness of the developing resist surface will exhibit correlation due to the underlying development rate correlations. But as development proceeds, parallel surface correlations will grow according to equation (17). At times and length scales where the parallel correlation length sufficiently exceeds the correlation length of the underlying roughness, Family-Viscek scaling will become manifest. This can also be seen from plots of the surface power spectral density as a function of development time. Figure 10 shows an example after 186 seconds of development (corresponding to 129 nm of resist removed) for case of $\xi = 15$ nm. Equation (18) fits the PSD well for $f < 1/(2\pi\xi)$, using the same $s = 0.93$ as for the uncorrelated case. Higher frequencies, corresponding to length scales less than ξ , show a greater slope, with $\alpha \approx 0.7$, though an accurate determination of α is difficult.

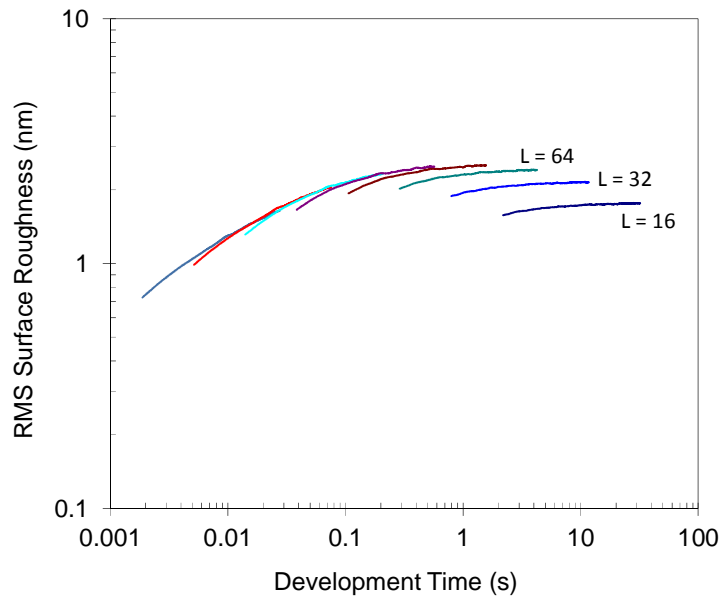


Figure 9. Scaled dynamic roughening 2D simulations with the top 80 nm of resist thickness data removed (shown here for $\mu = 0.73$, $\sigma_m = 0.03$, and $n = 10$ and for a protecting group correlation length of 15 nm). Data shown is the average of 1000 trials.

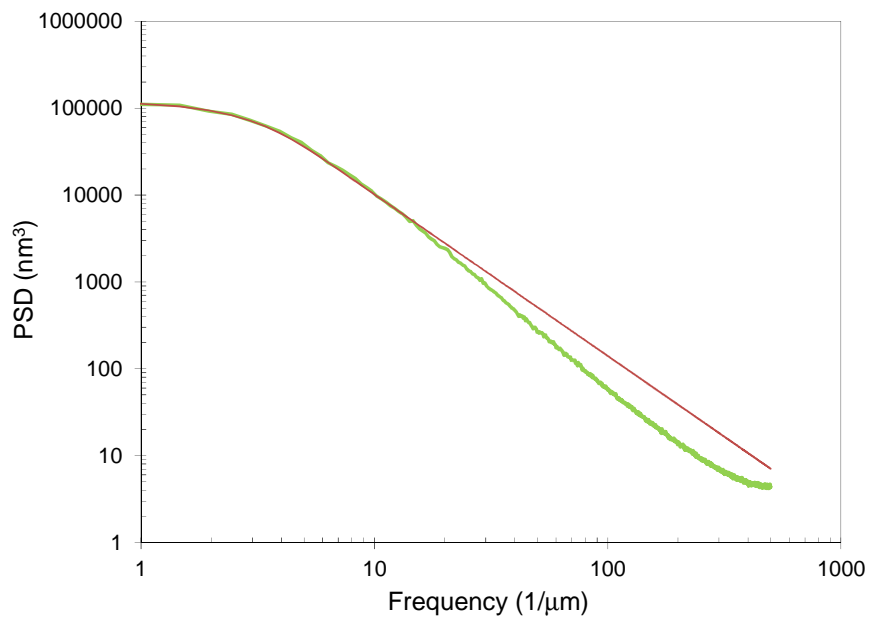


Figure 10. PSD after 186 s of development, corresponding to a depth of 129 nm into the resist ($\mu = 0.73$, $\sigma_m = 0.03$, $n = 10$, and a protecting group correlation length of 15 nm), with a fit shown as the thin red line. Data shown is the average of 1600 trials.

5. Conclusions

Previous work has shown that uncorrelated Gaussian randomness in the development rate produces surface roughness in a resist that obeys Family-Viscek scaling in the KPZ universality class. The use of a heavily skewed but uncorrelated development rate probability function, a result of a high dissolution selectivity n , does not change this result. Once correlation is added to the spatial distribution of development rates, however, the dynamical scaling becomes anomalous.

By carrying out 1+1 simulations of resist development under varying amounts of correlated development rate randomness, a transition between anomalous and KPZ scaling was observed. For length scales greater than about 5ξ , both along the surface and with depth into the resist, the dynamical roughness behavior obeys standard Family-Viscek scaling within the KPZ universality class. For length scales on the order of a few ξ or less, the mixed correlations of both ξ and ξ_{\parallel} make the results anomalous. In this regime, both α and β are higher than the KPZ values. It appears that correlations can explain at least some of the anomalous scaling behavior observed previously by Constantoudis⁸.

So far, all simulations have assumed a simulated volume with a uniform value of μ (that is, no gradients in exposure). Future work will add gradients, such as are found near a line edge, to understand their effect on the dynamic roughening process.

¹ G. Gallatin, "Resist Blur and Line Edge Roughness", *Optical Microlithography XVIII, Proc.*, SPIE Vol. 5754, pp. 38-52 (2004).

² A. Saeki, T. Kozawa, S. Tagawa, H. Cao, H. Deng, M. Leeson, "Exposure dose dependence on line edge roughness of a latent image in electron beam/extreme ultraviolet lithographies studied by Monte Carlo technique", *J. Micro/Nanolith. MEMS MOEMS*, **6**, p. 043004 (2007).

³ Gerard M. Schmid, Michael D. Stewart, Sean D. Burns, and C. Grant Willson, "Mesoscale Monte Carlo Simulation of Photoresist Processing," *J. Electrochem. Soc.*, **151**, pp. G155-G161 (2004).

⁴ C. A. Mack, John J. Biafore, and Mark D. Smith, "Stochastic Acid-Base Quenching in Chemically Amplified Photoresists: A Simulation Study", *Advances in Resist Technology and Processing XXVIII, Proc.*, SPIE Vol. 7972, p. 79720V (2011).

⁵ C. A. Mack, James W. Thackeray, John J. Biafore, and Mark D. Smith, "Stochastic Exposure Kinetics of EUV Photoresists: A Simulation Study", *Journal of Micro/Nanolithography, MEMS, and MOEMS*, Vol. 10, No. 3, p. 033019 (Jul-Sep, 2011).

⁶ C. A. Mack, "Stochastic Modeling in Lithography: The Use of Dynamical Scaling in Photoresist Development", *Journal of Micro/Nanolithography, MEMS, and MOEMS*, Vol. 8, No. 3, p. 033001 (Jul-Sep 2009).

⁷ C. A. Mack, "Stochastic modeling of photoresist development in two and three dimensions", *Journal of Micro/Nanolithography, MEMS, and MOEMS*, Vol. 9, No. 4, p. 041202 (Oct-Dec, 2010).

⁸ Vassilios Constantoudis, George P. Patsis, and Evangelos Gogolides, "Evolution of resist roughness during development: stochastic simulation and dynamic scaling analysis", *J. Micro/Nanolith. MEMS MOEMS*, **9**, 041207 (2010).

⁹ C. A. Mack, *Fundamental Principles of Optical Lithography*, John Wiley & Sons, London, p. 260 (2007).

¹⁰ C. A. Mack, "Stochastic Modeling in Lithography: Autocorrelation Behavior of Catalytic Reaction-Diffusion Systems", *Journal of Micro/Nanolithography, MEMS, and MOEMS*, Vol. 8, No. 2, p. 029701 (Apr-Jun 2009).

¹¹ R. L. Stratonovich, *Topics in the Theory of Random Noise, Volume I*, Gordon & Breach, New York, p. 22 (1963).

¹² Eric I. Thorsos, "The validity of the Kirchhoff approximation for rough surface scattering using a Gaussian roughness spectrum", *J. Acoust. Soc. Am.* **83** (1), p. 78-92 (Jan. 1988).

¹³ F. Family and T. Vicsek, "Scaling of the active zone in Eden process on percolation networks and the ballistic deposition model", *J. Phys. A: Math. Gen.*, Vol. 18, pp. L75-81 (1985).